Experimental Feasibility of Breast Tumor Detection and Localization

Elise C. Fear+, Jeff Sill+, and Maria A. Stuchly*

+University of Calgary, Electrical & Computer Engineering, 2500 University Dr. NW, Calgary, AB, T2N 1N4,
*University of Victoria, Electrical & Computer Engineering, BOX 3055, STN CSC, Victoria, BC, V8W 3P6

ABSTRACT — **Microwave breast imaging with radar-based techniques has been proposed for breast tumor detection. The feasibility study reported in this paper is designed to evaluate detection and localization of objects in three dimensions (3D). Experimental setups consisting of a PVC pipe (skin) and wood spheres (tumors) are illuminated with a resistively loaded monopole antenna. Improved image reconstruction algorithms are applied to the measured data, and the resulting images demonstrate detection and localization of smaller 3D tumor models.**

I. Introduction

A new method of breast cancer imaging with microwaves was proposed by Hagness in 1998 [1], [2]. In this configuration an antenna is scanned into various locations on a naturally flattened breast. Subsequently, Fear and Stuchly explored a cylindrical scanning system with the breast pendulant in a lossless liquid [3], [4]. This system is more compatible with clinical practice. However, an additional challenge is presented due to very large reflections from the skin. The physical basis of breast tumor detection with microwaves is the contrast in the electrical properties of normal and malignant breast tissues. Both systems employ wideband pulses and computational focusing of the microwave beam. The method is similar to that used in ground penetrating radar. Much work to date has involved computer simulations for concept verification [1]-[4]. Initial experimental feasibility testing with measurements of simple 2D phantoms is reported in [5].

In this contribution, the 2D experiments reported in [5] are extended to 3D. The system investigated in is referred to as TSAR (tissue sensing adaptive radar). The name is associated with image reconstruction algorithms that sense all tissues in the imaged volume and adapt to this information. Specifically, the skin is sensed first, and knowledge of the skin location and thickness modifies the tumor detection component of the imaging algorithm. An overview of the experiment and the improved image formation algorithms are described.

II. Experimental System

The experimental arrangements are similar to the one described in [5]. A resistively loaded monopole antenna is used to illuminate a PVC pipe containing a tumor model. The planes cutting through the PVC pipe perpendicular and parallel to its axis are imaged. Image plane 1 refers to the plane oriented perpendicular to the axis, while image plane 2 refers to the plane oriented parallel to the pipe axis. The system arrangement for the monopole antenna is shown in Fig. 1. Data for image plane 1 are acquired by rotating the model in 16 increments spaced by 22.5^0. This represents physically scanning the antenna around the phantom. For image plane 2, Figs. 1c and 1d show half of a PVC pipe placed on the ground plane. The tumor model is scanned past the antenna (inside of the pipe) to create the synthetic array. Measurements are taken at 21 locations spaced by 2.5 cm.

In all experiments, S_{11} reflections are recorded with an 8720C vector network analyzer (Agilent Technologies, Palo Alto, CA, USA) connected to a 50-ohm coaxial cable. To reduce ambient reflections, CRAM SFC high performance absorbers (Cuming Corporation, Avon, MA, USA) surround the setup. Data are recorded at 401 frequency points and 128 samples are averaged at each frequency. The frequency range, in which the data are acquired, is from 50 MHz to 20 GHz.

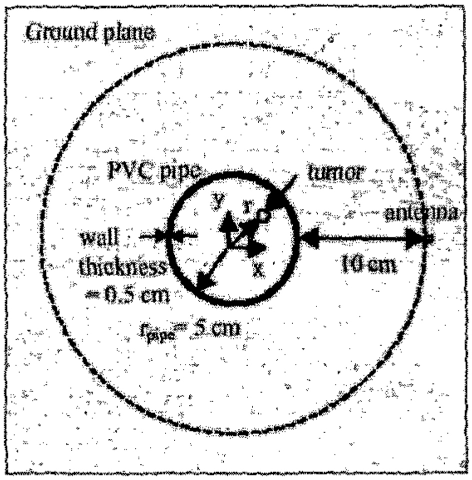

a)

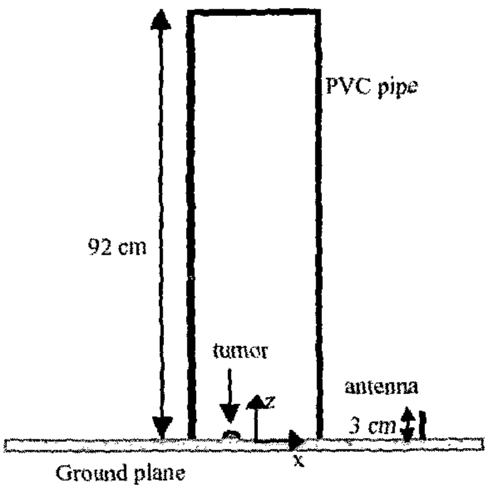

b)

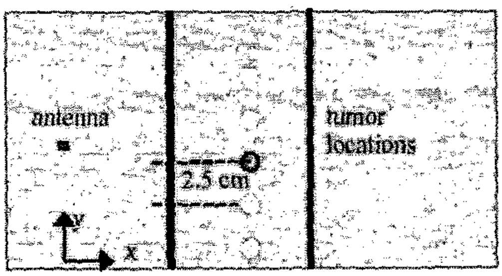

c)

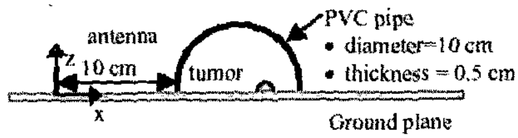

d)

Fig. 1. Experimental arrangement

A highly simplified model of the breast consists of a PVC pipe in which wooden hemispheres of diameters 1.25 and 2.5 cm are placed. The PVC pipe represents skin, the spheres represent tumors, and breast tissue is represented by air. The literature indicates properties of PVC at 15 GHz as relative dielectric constant ε_r= 2.9 and conductivity σ=0.01 S/m. Based on the known thickness of the pipe walls and time delay of the signal determined in our test, the permittivity of PVC in our experiments is estimated as ε_r=4. Properties of various types of wood change significantly with variations in moisture content. In order to characterize the material used for the tumor model, properties are measured in an X-band waveguide using the transmission-reflection method. The measured relative dielectric constant is 2.2 for the wood. The Plexiglas dielectric constant based on literature is 2.6. Simulations reported in [1]-[4] used the following properties for tissues: breast tissue with ε_r=9, σ=0.4 S/m; skin with ε_r=36, σ=4 S/m; and tumor with ε_r=50, σ=4 S/m. Comparing simulated and experimental models, the dielectric contrast between PVC and air is similar to the contrast between the dielectric constant of skin and breast tissues. In the phantom model, the contrast between PVC and wood is less than expected for the contrast between skin and tumor. Lossy breast tissue is not included in the phantom, so a tumor model of reduced contrast attempts to compensate for this effect.

III. Image Formation

The image formation algorithms are similar to those presented in [5]. The first step transforms the measured frequency-domain data to the time domain. A weighting is applied to create a differentiated Gaussian pulse with center frequency of 5.24 GHz and full-width half-maximum (FWHM) bandwidth from 1.68 to 10.6 GHz. The weighting is followed by an inverse chirp-z transform to convert the frequency domain data to the time domain. Calibration, subtraction of signals recorded with and without the phantom present, reduces the initial pulse and reflections from the antenna/feed mismatch. The dominant components of this signal are reflections from the pipe interfaces furthest from and closest to the antenna (Fig. 1). An initial image is formed by scanning the synthetic focus of the array through the region of interest with the time-shift and sum approach [4]. The PVC pipe is the dominant object in this initial image. The location of the pipe relative to each antenna is determined using thresholding. Time-gating is applied to eliminate the reflection from pipe interface 2, as well as reflections arriving before the first pipe reflection. Although data are limited to the first pipe reflection and reflections from model interior, the dominant reflection from the pipe must be reduced to permit tumor detection.

A modified subtraction method provides better cancellation of the pipe reflection compared to previously introduced algorithms [4]. The average phase shift between signals is used to align the dominant reflections, and then the average of this aligned set of signals is subtracted from all signals. The modified algorithm employs a version of Woody averaging [6], and essentially uses adaptive correlation to compute an average response for each antenna. After subtracting the estimated pipe reflection, image formation proceeds as described in [5], except for a different compensation of radial spreading. The final image created with the monopole antenna includes the area bounded by the antenna array for image plane 1, and the area bounded by the array and the second pipe interface for image plane 2.

IV. Results

[may want to add 2.5 cm diameter tumor image and planar image of 1.25 cm diameter tumor]

An image of tumor models having 1.25 cm diameter in plane 1 is shown in Fig. 2. Although the tumor is the dominant response in the image, significant clutter is present. In this case, the signal to clutter ratio is 2.0 dB. The tumor location is 2.7 cm compared with actual 2.9 cm. The image in Fig. 2 also illustrates the ability to detect the skin model and determine its shape and thickness (in practice, the skin outline and thickness).

Because of the difference in the dielectric constant the 1.25 cm size of the tumor model scales to 2.6 mm tissue tumor.

Figure 4 further illustrates tumor detection in with the monopole antenna, showing the image in plane 2. The signal to clutter ratio is in this plane 3 dB. The localization in plane 2 can further be improved if more antenna positions are used.

Fig. 2. Image of a 1.25 cm diameter tumor model

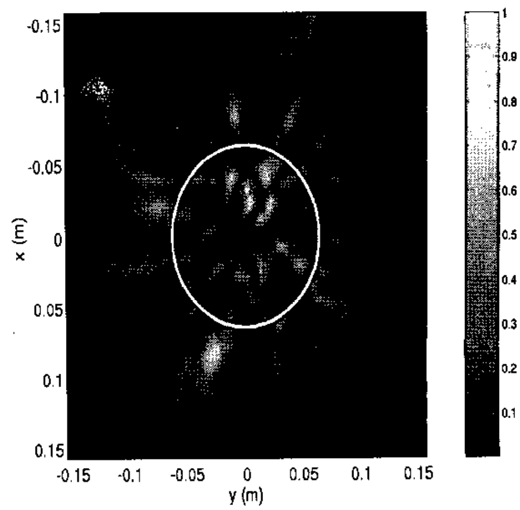

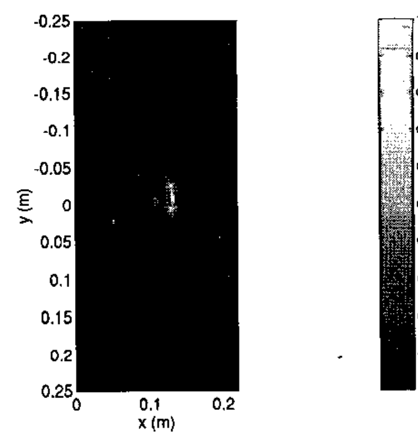

Fig. 4. Image of wooden tumor in plane 2; 21 locations of the monopole antenna.

V. Conclusions

The feasibility of experimentally detecting three-dimensional tumor models is confirmed. Tumor models are detected and localized in two planes, one in which the antennas encircle the phantom and one in which the antennas are scanned along the axis of the PVC pipe (skin). To obtain reasonable 3D localization, an antenna with narrower beam width than the monopole is required. Illuminating the entire object reduces the effectiveness of focusing. For reliable detection of smaller objects or detecting objects in complex environments, a higher gain antenna is desirable.

For all images, the TSAR imaging algorithm, which combines Woody averaging and time-gating to reduce reflections from the skin, provides an extremely simple and effective method of tumor detection. Future research into developing an appropriate antenna, as well as a realistic breast model with more representative shape, size, features and electrical properties is needed.

ACKNOWLEDGMENT

This research was supported by grants from the Natural Sciences and Engineering Research Council (NSERC) of Canada.

REFERENCES

[1] S. C. Hagness, A. Taflove, and J. E. Bridges, "Two-dimensional FDTD analysis of a pulsed microwave confocal system for breast cancer detection: Fixed-focus and antenna-array sensors," *IEEE Trans. Biomed. Eng.*, vol. 45, pp. 1470-1479, Dec. 1998.

[2] S. C. Hagness, A. Taflove, and J. E. Bridges, "Three-dimensional FDTD analysis of a pulsed microwave confocal system for breast cancer detection: Design of an antenna-array element," *IEEE Trans. Antennas Propag.*, vol. 47, pp. 783-791, May 1999

[3] E.C. Fear and M. A. Stuchly, "Microwave system for breast tumor detection", *IEEE Microwave and Guided Letters*, vol. 9, pp. 470-472, 1999.

[4] E.C. Fear and M. A. Stuchly, "Microwave system for breast tumor detection", *IEEE Trans. Microwave Theory and Techniques"*, vol. 48, pp. 1854-1863, 2000.

[5] E.C. Fear, J. Sill and M.A. Stuchly, "Experimental feasibility study of confocal microwave imaging", *IEEE Trans. Microwave Theory Tech.*, to appear March 2003.

[6] C.D. Woody, "Characterisation of an adaptive filter for the analysis of variable latency neuroelectric signals", *Medical Biological Eng.*, vol. 5, pp. 539-553, 1967.